*Journal of Clinical and Translational Hepatology* **2023** vol. 11(2) | 261–272
DOI: 10.14218/JCTH.2022.00042

Original Article

# RASAL2 Deficiency Attenuates Hepatic Steatosis by Promoting Hepatic VLDL Secretion via the AKT/TET1/MTTP Axis

Hao Ding[1#], Jiang-Hong Yu[1,2#], Ge Ge[3], Yan-Yun Ma[4,5,6], Jiu-Cun Wang[4], Jun Zhang[1*] and Jie Liu[1*]

*[1]Department of Digestive Diseases, Huashan Hospital, Fudan University, Shanghai, China; [2]Institutes of Biomedical Sciences, Fudan University, Shanghai, China; [3]Department of Dermatology, The Seventh Medical Center of PLA General Hospital, Beijing, China; [4]Human Phenome Institute, Fudan University, Shanghai, China; [5]Ministry of Education Key Laboratory of Contemporary Anthropology and State Key Laboratory of Genetic Engineering, School of Life Sciences, Fudan University, Shanghai, China; [6]Six-sector Industrial Research Institute, Fudan University, Shanghai, China*

**Received:** 28 January 2022 | **Revised:** 3 May 2022 | **Accepted:** 10 May 2022 | **Published:** 1 June 2022

## Abstract

***Background and Aims:*** RAS protein activator like 2 (RASAL2) is a newly discovered metabolic regulator involved in energy homeostasis and adipogenesis. However, whether RASAL2 is involved in hepatic lipid metabolism remains undetermined. This study explored the function of RASAL2 and elucidated its potential mechanisms in nonalcoholic fatty liver disease (NAFLD). ***Methods:*** NAFLD models were established either by feeding mice a high-fat diet or by incubation of hepatocytes with 1 mM free fatty acids (oleic acid:palmitic acid=2:1). Pathological changes were observed by hematoxylin and eosin staining. Lipid accumulation was assessed by Oil Red O staining, BODIPY493/503 staining, and triglyceride quantification. The *in vivo* secretion rate of very low-density lipoprotein was determined by intravenous injection of tyloxapol. Gene regulation was analyzed by chromatin immunoprecipitation assays and hydroxymethylated DNA immunoprecipitation combined with real-time polymerase chain reaction. ***Results:*** RASAL2 deficiency ameliorated hepatic steatosis both *in vivo* and *in vitro*. Mechanistically, RASAL2 deficiency upregulated hepatic TET1 expression by activating the AKT signaling pathway and thereby promoted MTTP expression by DNA hydroxymethylation, leading to increased production and secretion of very low-density lipoprotein, which is the major carrier of triglycerides exported from the liver to distal tissues. ***Conclusions:*** Our study reports the first evidence that RASAL2 deficiency ameliorates hepatic steatosis by regulating lipid metabolism through the AKT/TET1/MTTP axis. These findings will help understand the pathogenesis of NAFLD and highlight the potency of RASAL2 as a new molecular target for NAFLD.

**Citation of this article:** Ding H, Yu JH, Ge G, Ma YY, Wang JC, Zhang J, *et al*. RASAL2 Deficiency Attenuates Hepatic Steatosis by Promoting Hepatic VLDL Secretion via the AKT/TET1/MTTP Axis. J Clin Transl Hepatol 2023;11(2):261–272. doi: 10.14218/JCTH.2022.00042.

## Introduction

Nonalcoholic fatty liver disease (NAFLD) includes a group of chronic liver disorders ranging from simple steatosis to steatohepatitis and ultimately to cirrhosis.[1] Estimates indicate that 25.24% of the world's population has NAFLD.[2] In China alone, the number of NAFLD cases is estimated at 243 million in 2016 and is expected to grow to 314 million in 2030.[3] With its increasing prevalence, NAFLD has emerged as the most common chronic liver disease, and is expected to be the leading cause of liver transplantation by 2030.[4,5] However, due to a lack of understanding of its pathogenesis, there is currently no effective pharmacotherapy available for the treatment of NAFLD.

RAS protein activator like 2 (RASAL2) is a 142 kDa protein belonging to the Synaptic GTPase-activating protein family of Ras GTPase-activating proteins, which negatively regulate Ras function by enhancing GTPase activity and promoting the transition from activated Ras-GTP to inactive Ras-GDP.[6] Previous studies of RASAL2 focused primarily on tumors, including ovarian, bladder, renal, breast, and colorectal cancers.[7–11] Since 2009, a single nucleotide polymorphism near the RASAL2 gene, rs10913469, has been reported to be consistently associated with obesity in various ethnic populations.[12–14] Zhu *et al*.[15] found that *Rasal2* deficiency repressed adipogenesis by augmenting Ras activity and it attenuates high-fat diet-induced obesity and related metabolic disorders, including hepatic steatosis. The findings indicate that

**Keywords:** Nonalcoholic fatty liver disease; RASAL2; Very low-density lipoprotein; Steatosis; Lipid metabolism.

**Abbreviations:** 5-hmc, 5-hydroxymethylcytosine; 5-mc, 5-methylcytosine; ALT, alanine aminotransferase; AST, aspartate aminotransferase; BSA, bovine serum albumin; ChIP, chromatin immunoprecipitation; FBG, fasting blood glucose; FBI, fasting blood insulin; FFA, free fatty acids; HE, heterozygous; H&E, hematoxylin and eosin; HFD, high-fat diet; hMeDIP, hydroxymethylated DNA Immunoprecipitation; HO, homozygous; HOMA-IR, homeostasis model assessment of insulin resistance; NAFLD, nonalcoholic fatty liver disease; NCD, normal chow diet; PB, *piggyBac*; qRT-PCR, quantitative real-time polymerase chain reaction; RASAL2, RAS protein activator like 2; TC, total cholesterol; TG, triglycerides; VLDL, very low-density lipoprotein; WT, wild-type.

[#]Contributed equally to this work.

[*]**Correspondence to:** Jie Liu and Jun Zhang, Department of Digestive Diseases, Huashan Hospital, Fudan University, Shanghai 200040, China. ORCID: https://orcid.org/0000-0002-7638-187X (JL), https://orcid.org/0000-0002-9330-6070 (JZ). Tel: +86-21-52888236 (JL), +86-21-52888237 (JZ), Fax: +86-21-52888236, E-mail: jieliu@fudan.edu.cn (JL) and archsteed@163.com

RASAL2 acts as an important regulator of lipid metabolism. However, whether it is directly involved in NAFLD development and its specific molecular mechanisms remain undetermined. To address these issues, this study was conducted to clarify the specific role of RASAL2 in hepatic lipid metabolism both *in vitro* and *in vivo*, aiming to provide novel insights into the pathogenesis and treatment of NAFLD.

## Methods

### *Cell culture and treatment*

L02 and HepG2 cells were cultured in Dulbecco's minimal eagle medium containing 10% fetal bovine serum at 37°C in a 5% $CO_2$ humidified atmosphere. The *in vitro* model of NAFLD was induced by treatment with a mixture of 1 mM free fatty acids (FFA; oleic acid: palmitic acid = 2:1) containing 1% FFA-free bovine serum albumin (BSA) for 24 h as described by Gómez-Lechón *et al*.[16] Cells were transfected with RASAL2 overexpression plasmid (GV492-RASAL2: GeneChem, Shanghai, China; pNTAP-RASAL2: provided by Professor Wu Xiaohui of Fudan University) or siRNAs (siRASAL2: forward 5′-GCAGGACAGUUCAACCUAATT-3′; siTET1: forward 5′-CCUCCAGUAAUGGCUAUAATT-3′; Scrambled: forward 5′-UUCUCCGAACGUGUCACGUTT-3′; Biotend, Shanghai, China), followed by FFA treatment with or without AKT inhibitor triciribine and MEK inhibitor U0126 (both from Apexbio, Houston, TX, USA) for 24 h.

### *Experimental animals*

The founder *Rasal2*$^{PB/+}$ mice were generated by the *piggyBac* (PB) transposon, which was inserted into the intron region between exon 2 and exon 3 on the FVB/NJ background and was kindly donated by Professor Wu Xiaohui of Fudan University. The wild-type (WT), heterozygous (HE), and homozygous (HO) genotypes were identified by PCR assays of DNA obtained by tail biopsies at 2–3 weeks. The primer sequences used were WT forward: TCCTAAGTATATATGCCGATTAAAA; common: TGAGGACTTACACCCCCAGT; mutant forward: CT GAGATGTCCTAAATGCACAGC. The expected amplicon sizes were (1) WT, 235 bp; (2) HE, 235 bp and 310 bp, and (3) HO, 310 bp. At 4–5 weeks of age, male mice were divided into four groups of six mice each. WT littermates were used as controls. The mice were fed a normal chow diet (NCD, D12450B) or a high-fat diet (HFD, D12492; both from Research Diets, NJ, USA) for 12 weeks. All animal study protocols were approved by the Committee on the Ethics of Animal Experiments of Fudan University and implemented according to the National Institutes of Health Guide for the Care and Use of Laboratory Animals.

### *Sample collection*

At the end of the study, mice were fasted overnight, intraperitoneally anesthetized with sodium pentobarbitone at 80 mg/kg, and sacrificed by exsanguination. Blood plasma was obtained by centrifugation and stored at −80°C until use. A portion of each liver was fixed in 4% neutral-buffered paraformaldehyde, and the remaining tissue was immediately frozen in liquid nitrogen for subsequent use.

### *Human liver samples*

Given the difficulty of obtaining liver specimens from healthy individuals and non-cancer NAFLD patients for obvious ethical reasons, we collected surgically resected liver tissue from patients with hepatocellular carcinoma. Adjacent noncancerous tissues (six steatosis and six normal) were used for subsequent studies. Patients with an alcohol intake of >20 g per day, infections of hepatitis-related viruses or human immunodeficiency virus, receiving potentially hepatotoxic drugs, and other causes of chronic liver disease were excluded. All tissue samples were obtained with informed consent following Institutional Review Board approval and following the ethical guidelines of the Declaration of Helsinki.

### *Microarray data analysis*

Dataset GSE48452 was downloaded from the Gene Expression Omnibus database (http://www.ncbi.nlm.nih.gov/geo/). The microarray data were annotated by matching with the GPL11532 (HuGene-1_1-st) Affymetrix Human Gene 1.1 ST Array. Fourteen healthy controls and 32 NAFLD patients (14 steatosis and 18 steatohepatitis) were selected for further analysis.

### *Measurement of biochemical parameters in plasma*

The plasma levels of triglycerides (TG), total cholesterol (TC), fasting blood glucose (FBG), alanine aminotransferase (ALT), and aspartate aminotransferase (AST) were determined with a biochemical autoanalyzer. Fasting blood insulin (FBI) was measured with an Ultrasensitive Mouse Insulin ELISA Kit (90080, Crystal Chem, IL, USA) following the manufacturer's instructions. The homeostasis model assessment of insulin resistance (HOMA-IR) was quantified as HOMA-IR=FBG (mmol/L) × FBI (mIU/L)]/22.5.

### *In vivo very low-density lipoprotein (VLDL) secretion assay*

The VLDL secretion rate was determined as previously reported.[17] Briefly, mice were fasted for 8 h and then received intravenous tail vein injections of tyloxapol (sc-255711; Santa Cruz Biotechnology, Dallas, TX, USA) at 500 mg/kg in PBS. Blood sampling was performed at 0, 1, 2, and 3 h after tyloxapol injection. The secretion rate *in vivo* was calculated from the slope of the plasma TG accumulation over time by linear regression analysis.

### *Histological analyses and immunohistochemistry*

Hepatic histopathology was studied with hematoxylin and eosin (H&E) and Oil Red O staining. The expression and localization of RASAL2 were investigated by immunohistochemistry. Slides were visualized by light microscopy (Nikon, Tokyo, Japan). All microscopic examinations were performed by the same researcher blinded to treatment assignments. The Oil Red O-stained area was calculated as a percentage of the total section by Image-Pro Plus v6.0 software (Media Cybernetics, MD, USA).

### *Hepatic and cellular TG quantification*

Hepatic and cellular TG were assayed with a TG determination kit (E1013; Applygen Technologies Inc., Beijing, China). TG levels were normalized to the total protein concentration

with a bicinchoninic acid assay kit (23225; Thermo Fisher Scientific, Waltham, MA, USA).

### *Immunofluorescence staining*

Immunofluorescence staining was performed on cells cultured on cover slips. The cells were washed twice with PBS, fixed with 4% paraformaldehyde and permeabilized with 0.25% Triton X-100. Slides were blocked with 5% BSA and stained with anti-RASAL2 primary antibody (1:300; 22140; Proteintech, Wuhan, China) followed by incubation with Cy3 conjugated secondary antibody (1:200; GB21403; Servicebio, Wuhan, China) and BODIPY493/503 (1 μg/mL; Thermo Fisher Scientific). 4′,6-diamidino-2-phenylindole was used to counterstain the nuclei. The slides were visualized and photographed with a fluorescence microscope (Nikon, Tokyo, Japan).

### *Quantitative real-time polymerase chain reaction (qRT-PCR)*

TRIzol (15596018; Thermo Fisher Scientific) was used to extract the total RNA. cDNA was synthesized with a high-capacity RNA-to-cDNA Kit (4388950; Applied Biosystems, Hercules, CA, USA) and was assayed by qRT-PCR using SYBR Green master mix (A25780; Thermo Fisher Scientific) on a LightCycler 480 II Instrument (Roche, Burgess Hill, UK). The expression the target genes was normalized to GAPDH. The primer sequences used in this study are listed in Supplementary Table 1.

### *Western blot assay*

Total protein was extracted with RIPA lysis buffer with protease/phosphatase inhibitors. Protein samples were quantified by bicinchoninic acid assay method, separated by sodium dodecyl-sulfate polyacrylamide gel electrophoresis and transferred to polyvinylidene difluoride membranes. The primary antibodies were against RASAL2 (22140, Proteintech; Santa Cruz Biotechnology, 390605), CPT1A (15184, Proteintech), ACOX1 (10957, Proteintech), p-ERK1/2 (4370; Cell Signaling Technology, Danvers, MA, USA), p-AKT (4060, Cell Signaling Technology), TET1 (293186, Santa Cruz Biotechnology; 124207, GeneTex, Irvine, CA, USA), MTTP (515742, Santa Cruz Biotechnology), and GAPDH (30201ES20, Yeasen, Shanghai, China).

### *VLDL content determination*

VLDL was determined using an ELISA kit (RK02508; ABclonal, Wuhan, China). Briefly, the cell culture medium was collected after treatment and then centrifuged to remove debris. The cells were washed twice, harvested, and lysed in cell lysis buffer. The cell lysate and culture supernatant were used for the ELISA. The VLDL content in the cell lysate was normalized to the total protein level.

### *Dot blot*

Genomic DNA extraction was conducted using the TIANamp Genomic DNA Kit (DP304; Tiangen Biotech, Beijing, China). DNA was denatured and then spotted onto nitrocellulose membranes, which were dried at 80°C and UV-crosslinked for 15 minutes. The membrane was blocked with 5% BSA and incubated with primary antibodies against 5-methylcytosine (5-mC) (1:2,000; 10805; Abcam, Cambridge, UK) and 5-hydroxymethylcytosine (5-hmC) (1:1,000; 39069; Active Motif, Carlsbad, CA, USA) overnight. Horseradish peroxidase-conjugated secondary antibodies were used to probe the cells on the following day.

### *Chromatin immunoprecipitation (ChIP) assay*

ChIP was carried out using an EZ-magna ChIP A/G kit (17-10086; Millipore, Waltham, MA, USA). Nuclear extract preparation, immunoprecipitation, and DNA purification were performed following the manufacturer's instructions. Anti-TET1 antibody (61443; Active Motif) was used for immunoprecipitation. Anti-RNA polymerase II was a positive control, and normal rabbit IgG was a negative control. The DNA fragments were then purified and subjected to qRT-PCR for MTTP promoter detection. The primer sequences used were, -525 — -411: forward 5′-TCCCACTGATTCTTTGCAAACT-3′, reverse 5′-CCCGTCTCTGAAATGCGTTT-3′; -463 — -298: forward 5′-TCGCCCACTATCCCTTCTAG-3′, reverse 5′-CAGTGGTGTGGAAGTGGTTT-3′; -350 — -175: forward 5′-CGACGTCATTTCCTTCAGCA-3′, reverse 5′-TCAGCTCGGTAAGTGTCCTG-3′; -244 — -94: forward 5′-CCCCTTTGCGTCCAGAGAAT-3′, reverse 5′-TTCTGTGGAAGGAAGCGTGA-3′; -171 — -52: forward 5′-GTTGACAGGGAAGTGAAATCTCA-3′, reverse 5′-AGCCTCCACTGCGTAACTAC-3′; and -91 — +64: forward 5′-TTCAATTCCCAGAGGCAGG-3′, reverse 5′-CCTCCCACTCCCAAAACACT-3′.

### *Hydroxymethylated DNA Immunoprecipitation (hMeDIP)*

5-hmC immunoprecipitation was performed with EpiQuik hmeDIP kits (P-1038; Epigentek, Farmingdale, NY, USA). Genomic DNA was extracted and fragmented by sonication. DNA containing 5-hmC was enriched following the kit instructions. Nonimmune IgG was used as a negative control. The precipitated DNA was used as a template for qRT-PCR analysis.

### *Data and statistical analysis*

Statistical analysis was done with SPSS 22.0 (IBM Corp., Armonk NY, USA) and reported as means ± standard deviation. Between-group comparisons were conducted with Student's *t*-test, and multiple-group comparisons were conducted with one-way analysis of variance. *P*-values <0.05 were considered statistically significant.

## Results

### *Increased expression of RASAL2 in steatotic livers*

An *in vivo* model of NAFLD was established by HFD feeding for 12 weeks. Compared with normal livers, the protein levels of RASAL2 in the livers of HFD-fed mice were increased significantly (Fig. 1A). We next established a cellular model of NAFLD in L02 and HepG2 cells by treatment with a 1 mM FFA mixture and found a similar result to that observed in the mouse model (Fig. 1B). To validate the findings, the microarray chip data of GSE48452 were downloaded, and the results demonstrated that RSASAL2 gene expression was significantly increased in NAFLD patients (Fig. 1C). Immunohistochemistry analysis was performed on human liver sections and confirmed a significant elevation of RASAL2 in steatotic livers (Fig. 1D).

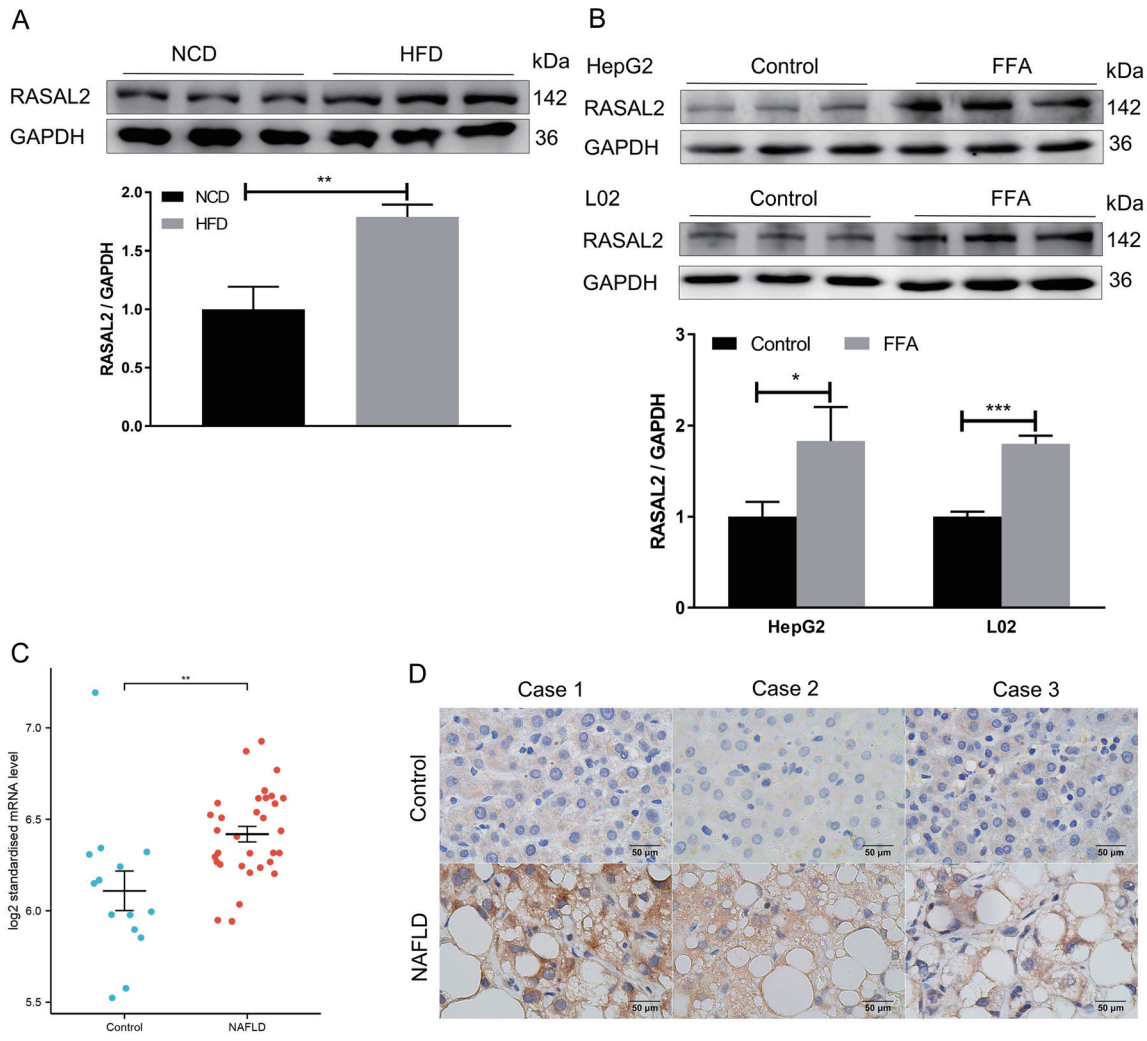


**Fig. 1. RAS protein activator like 2 (RASAL2) expression is upregulated in steatotic livers.** (A) RASAL2 expression in the livers of the normal chow diet (NCD)- and high-fat diet (HFD)-fed mice. (B) RASAL2 expression in free fatty acids (FFA)-treated hepatocytes. (C) Scatter plots of RASAL2 expression in the livers of nonsteatotic controls ($n$=14) and nonalcoholic fatty liver disease (NAFLD) patients (14 steatosis and 18 steatohepatitis) from the GSE48452 dataset. (D) Immunohistochemistry analysis (×400) of RASAL2 expression in noncancerous liver tissues of nonsteatotic donors ($n$=6) and patients with NAFLD ($n$=6). $^{*}p<0.05$, $^{**}p<0.01$, $^{***}p<0.001$.

### *RASAL2 deficiency ameliorates HFD-induced hepatic steatosis and metabolic disorders*

We next screened homozygous RASAL2-deficient mice by PCR using mouse tail genomic DNA and confirmed them by western blot analysis (Fig. 2A, B). As shown in Figure 2C–I, the body weight, plasma lipid profiles, FBG, FBI, ALT, AST, and hepatic TG contents were significantly increased after HFD feeding of both WT and *Rasal2*$^{PB/PB}$ mice. Compared with the WT littermates, RASAL2 deficiency significantly ameliorated HFD-induced hepatic steatosis (Fig. 2C, D, I), liver injury (Fig. 2H), and associated metabolic disorders, including obesity (Fig. 2E), hyperlipidemia (Fig. 2F), and insulin resistance (Fig. 2G). Notably, under NCD feeding conditions, *Rasal2*$^{PB/PB}$ mice had progressively less weight gain than their WT littermates, and the trend was much more pronounced under HFD feeding conditions (Fig. 2E). FBG levels were not significantly different between WT and *Rasal2*$^{PB/PB}$ mice, but FBI and HOMA-IR were significantly improved in *Rasal2*$^{PB/PB}$ mice fed a HFD, indicating an improvement in HFD-induced insulin resistance in RASAL2-deficient mice (Fig. 2G). These results are in agreement with those reported by Zhu *et al*.[15]

### *RASAL2 regulates lipid accumulation in FFA-treated hepatocytes*

To elucidate the specific role of RASAL2 in hepatic lipid metabolism, an *in vitro* NAFLD model was established in L02 and HepG2 cells by treatment with a 1 mM FFA mixture. As shown in Figure 3, knockdown of RASAL2 significantly alleviated lipid accumulation in FFA-treated hepatocytes, while overexpression of RASAL2 significantly aggravated lipid accumulation, as evidenced by intracellular TG quantification and immunofluorescence staining using BODIPY493/503.

### *RASAL2 deficiency upregulates the expression of MTTP in HFD-fed mice*

We next performed qRT-PCR analysis to examine the ex-

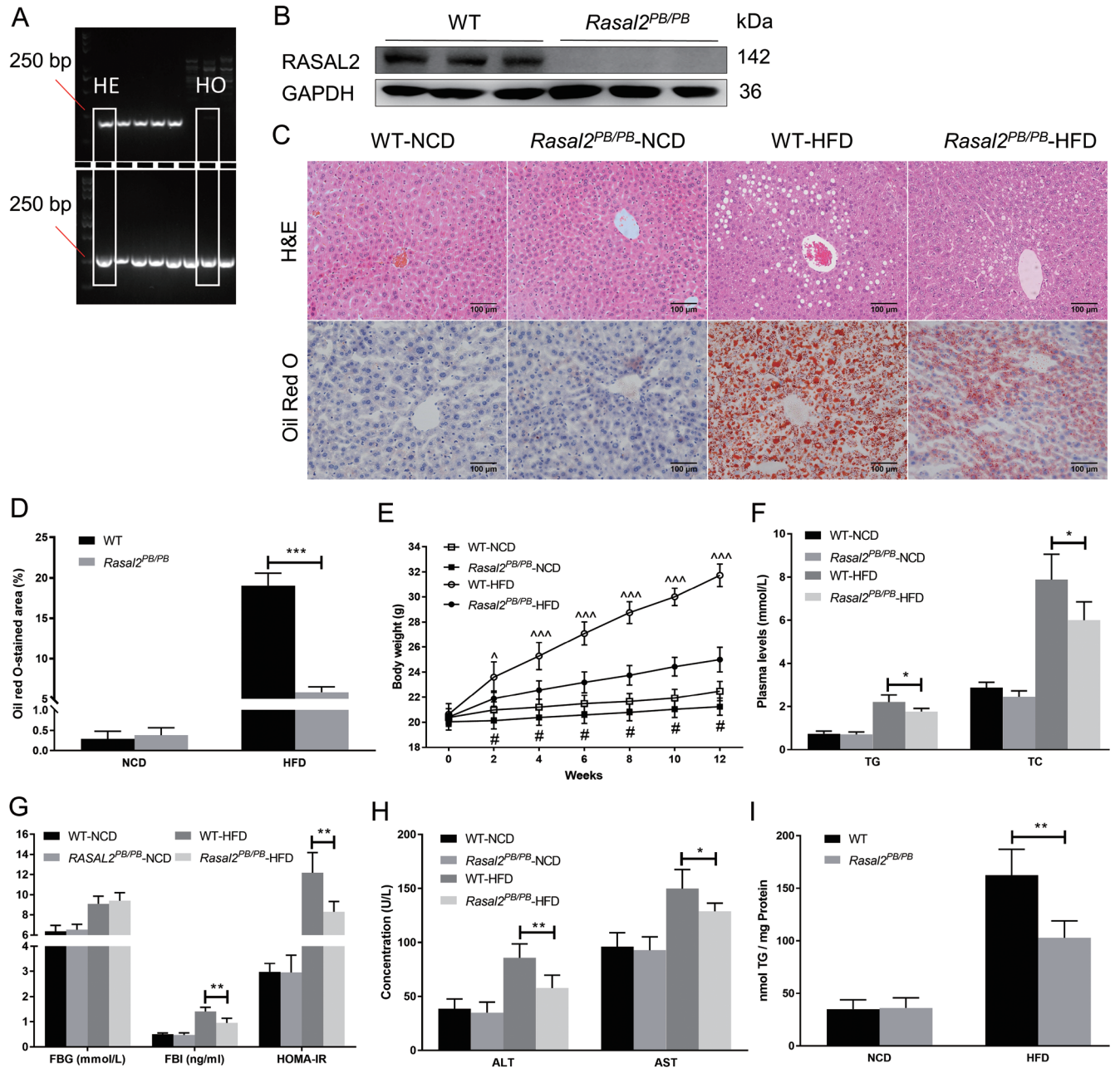


**Fig. 2. RAS protein activator like 2 (RASAL2) deficiency protects against hepatic steatosis and metabolic disorders in high-fat diet (HFD)-fed mice.** (A) PCR genotyping of wild-type (WT), heterozygous (HE), and homozygous (HO) RASAL2-deficient mice. (B) Confirmation of RASAL2 deficiency in the livers of RASAL2-deficient mice by western blot. (C) Hematoxylin and eosin (H&E) and Oil Red O staining showing reduced hepatic steatosis in the livers of RASAL2-deficient mice (×200). (D) Quantitation of the Oil Red O-stained area in liver sections. Body weight (E), plasma triglycerides (TG) and total cholesterol (TC) (F), fasting blood glucose (FBG) and fasting blood insulin (FBI) levels and homeostasis model assessment of insulin resistance (HOMA-IR) index (G), plasma alanine aminotransferase (ALT) and aspartate aminotransferase (AST) concentrations (H), and hepatic TG contents (I) in WT and RASAL2-deficient mice fed with normal chow diet (NCD) or HFD for 12 weeks. $^{\#}p<0.05$ versus the WT-NCD group. $^{\wedge}p<0.05$, $^{\wedge\wedge\wedge}p<0.001$ versus the *Rasal2*$^{PB/PB}$-HFD group. $^{*}p<0.05$, $^{**}p<0.01$.

pression levels of key genes involved in hepatic lipid homeostasis. Compared with WT littermates fed a HFD, expression of the lipid export-related gene *Mttp* and lipid oxidation-related genes *Acox1* and *Cpt1a* was significantly upregulated in the livers of diet-matched *Rasal2*$^{PB/PB}$ mice (Fig. 4A). Western blotting showed that only the expression of MTTP protein was significantly elevated in the livers of *Rasal2*$^{PB/PB}$ mice fed a HFD, while no significant differences in ACOX1 and CPT1A were observed (Fig. 4B).

### *RASAL2 deficiency increased the production and secretion of VLDL in HFD-fed mice and FFA-treated hepatocytes*

MTTP has a central role in VLDL assembly and secretion

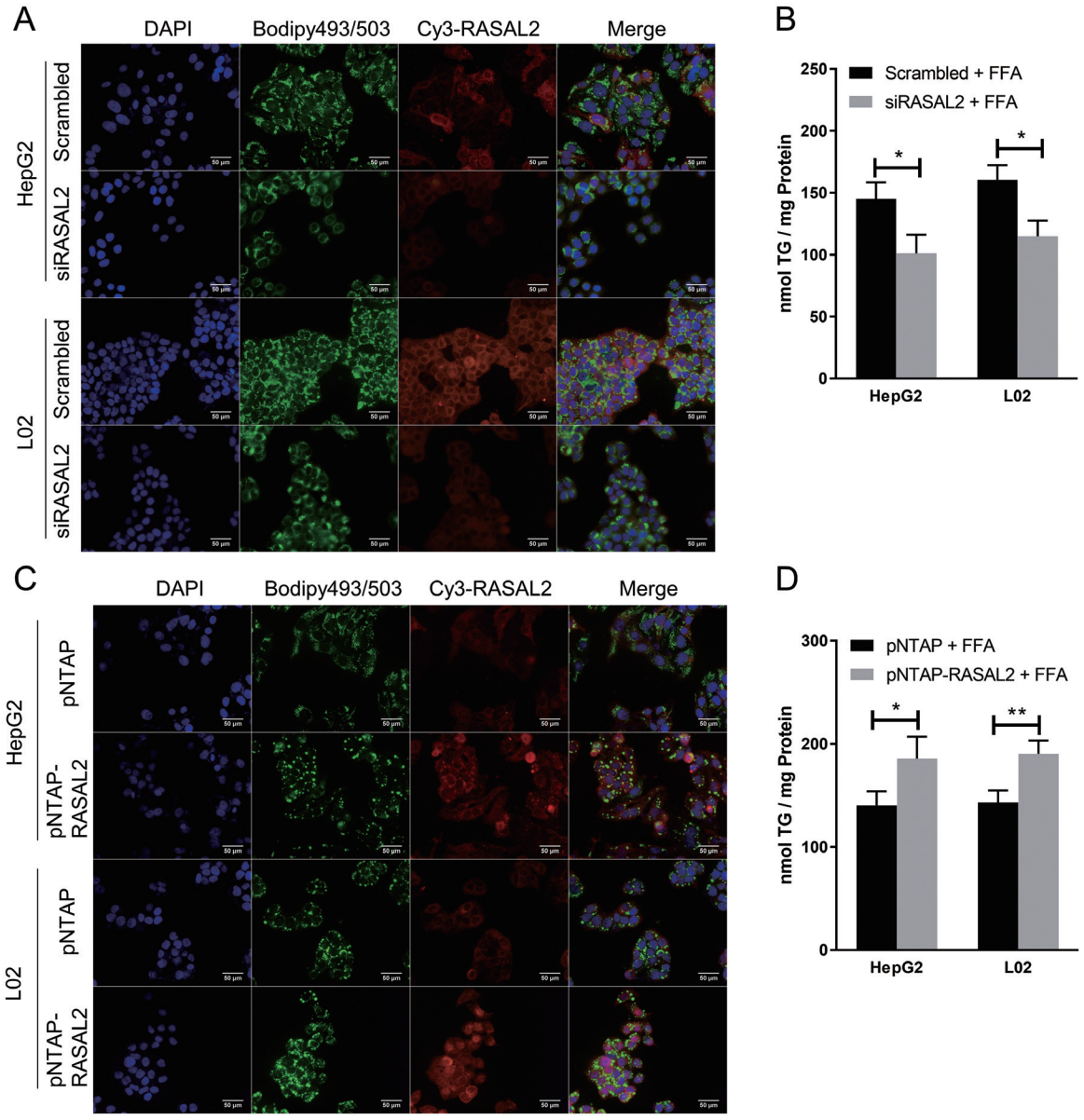


**Fig. 3. Effects of RAS protein activator like 2 (RASAL2) knockdown and overexpression on intracellular lipid accumulation in free fatty acids (FFA)-treated hepatocytes.** (A, C) Representative immunofluorescence images (×400) showing the effects of RASAL2 knockdown (A) or overexpression (C) on hepatic steatosis in cultured hepatocytes. (B, D) Measurement of intracellular triglycerides (TG) in hepatocytes with RASAL2 knockdown (B) or overexpression (D). $^{*}p<0.05$, $^{**}p<0.01$.

from hepatocytes.[18] Liver-specific knockout of *Mttp* led to a dramatic decrease in VLDL-TG.[19] Given the significant regulatory role of RASAL2 on MTTP expression, we examined whether RASAL2 could regulate the production and secretion of VLDL. In mice fed a HFD, tyloxapol was administered to block VLDL catabolism and clearance by inhibiting lipoprotein lipase activity to assess the *in vivo* rate of VLDL secretion. Compared with WT littermates, the levels of plasma TG in *Rasal2*$^{PB/PB}$ mice were significantly higher after tyloxapol injection, and the secretion rate of VLDL in *Rasal2*$^{PB/PB}$ mice was estimated to be approximately 1.98 times that in WT mice (Fig. 5A). Consistently, in FFA-treated hepatocytes, the intracellular and supernatant VLDL levels were significantly elevated after the knockdown of RASAL2 (Fig. 5B).

### *RASAL2 regulates MTTP expression by TET1-mediated DNA hydroxymethylation*

MTTP transcription has previously been reported to be regulated by DNA methylation.[20] We queried the UCSC Genome Browser database and found that the *MTTP* gene harbors a 557 bp CpG island in its promoter region; thus, we detected the gene expression of DNA methyltransferases and Tet family DNA demethylases in the livers of HFD-fed mice. The mRNA expression levels of the DNA methyltransferases *Dnmt1*, *Dnmt3a*, and *Dnmt3b* were not significantly changed, but *TET1* gene expression was significantly increased in *Rasal2*$^{PB/PB}$ mice (Fig. 6A). Western blot results further confirmed the upregulation of TET1 protein

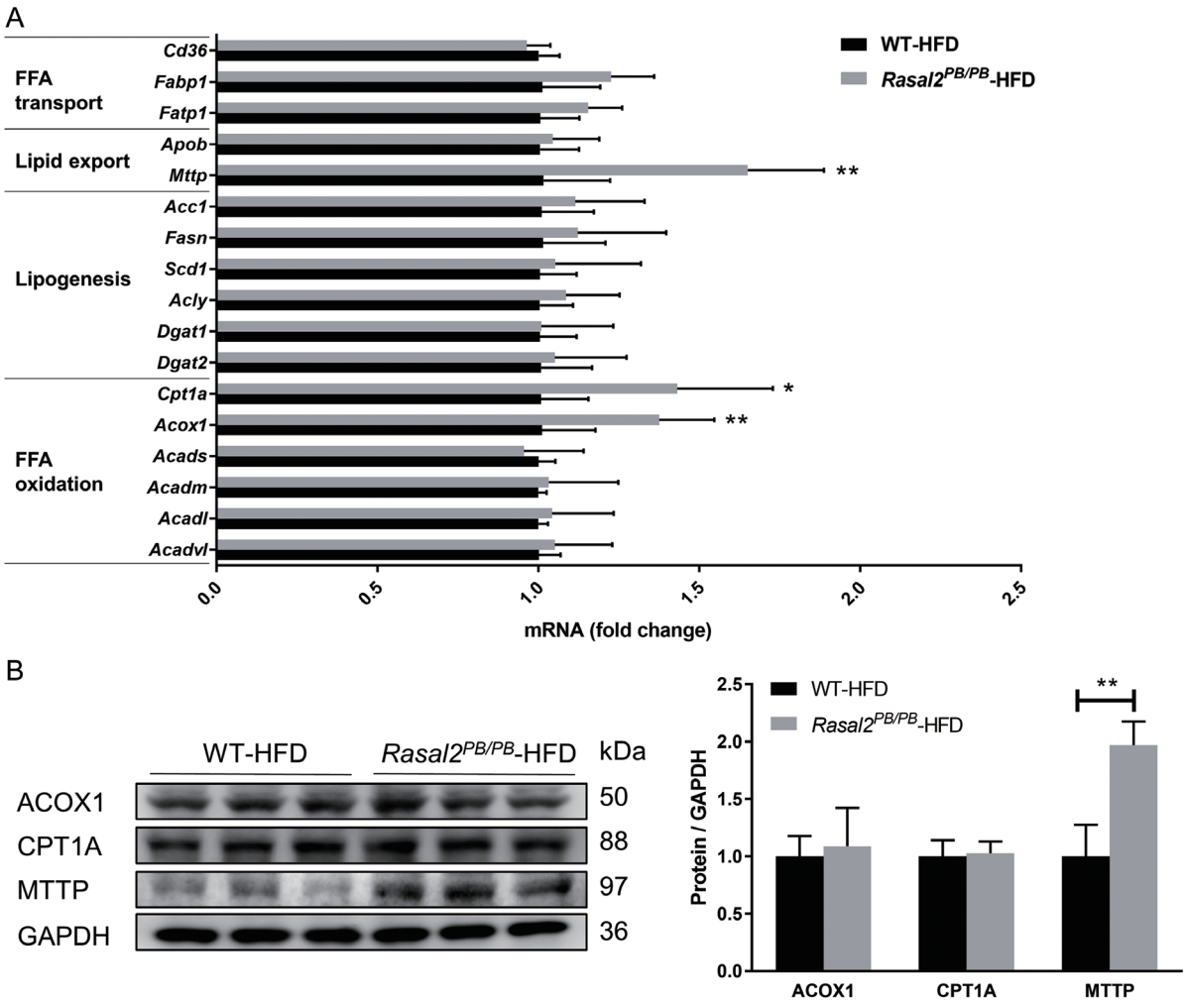


**Fig. 4. RAS protein activator like 2 (RASAL2) deficiency upregulates MTTP expression in the livers of high-fat diet (HFD)-fed mice.** (A) The mRNA expression of key genes related to lipid metabolism in the livers of HFD-fed mice. (B) Western blot analyses of ACOX1, CPT1A, and MTTP expression in the livers of HFD-fed mice. $^{*}p<0.05$, $^{**}p<0.01$, $^{***}p<0.001$.

expression in liver tissues of *Rasal2*$^{PB/PB}$ mice (Fig. 6B). In FFA-treated hepatocytes, the mRNA and protein expression levels of TET1 were also significantly elevated with RASAL2 knockdown (Fig. 6C and 6D). Furthermore, the effects of RASAL2 knockdown on increasing MTTP expression and promoting the production and secretion of VLDL were abrogated by the knockdown of TET1 (Fig. 6D and 7A).

As a DNA demethylase enzyme, TET1 mediates the transformation of 5-mC to 5-hmC, and TET1 overexpression decreased global DNA methylation and increased global 5-hmC levels in U2OS and HEK293T cells.[21] We performed dot blots to assess the global changes in 5-mC and 5-hmC *in vitro*. The results showed that the global levels of 5-mC were reduced and 5-hmC levels were elevated with RASAL2 knockdown (Fig. 7B, C). We then asked whether MTTP is a direct target of TET1 by performing a ChIP assay. It was found that TET1 directly bound to several segments within the *MTTP* promoter region, among which the strongest binding region was -171 — -52 bp (Fig. 7D). We conducted hMeDIP and tested for the presence of the -171 — -52 bp segment of the *MTTP* promoter in the enriched 5-hmC fractions by qRT-PCR, which showed that 5-hmC levels in the *MTTP* promoter region were significantly increased after RASAL2 knockdown in FFA-treated hepatocytes (Fig. 7E).

### *RASAL2 deficiency upregulates TET1 expression through the AKT signaling pathway*

As a member of the Ras GTPase-activating protein family, RASAL2 exerts its regulatory roles by modulating the Ras signaling pathway in various biological processes, including tumorigenesis, epithelial-mesenchymal transition, tumor metastasis, and adipogenesis.[15,22,23] We thus inhibited either the PI3K/AKT or the MAPK/ERK axis, two major downstream signaling pathways of Ras, with the small molecule inhibitors triciribine and U0126 to determine the specific pathway mediating TET1 upregulation by RASAL2 deficiency in cultured hepatocytes. Compared with FFA treatment alone, combined treatment with FFA and the AKT inhibitor triciribine significantly reduced the expression of TET1 mRNA in RASAL2 knockdown hepatocytes (Fig. 8A). Meanwhile, the phosphorylation levels of AKT were significantly increased after RASAL2 knockdown, and the upregulated protein expression levels of

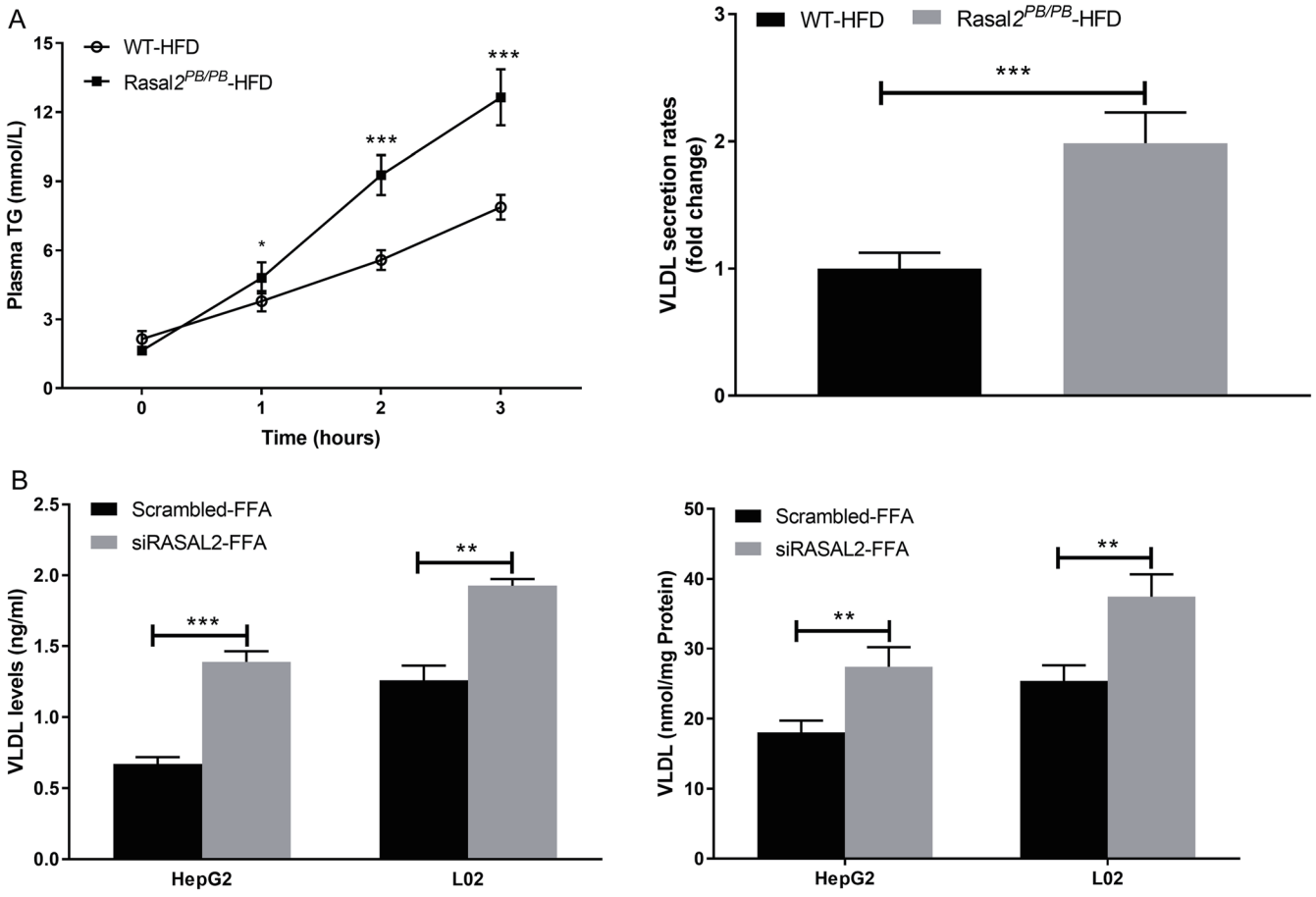


**Fig. 5. Effects of RAS protein activator like 2 (RASAL2) on hepatic very low-density lipoprotein (VLDL) production and secretion *in vivo* and *in vitro*.** (A) Plasma triglycerides (TG) determination after tyloxapol injection. The relative rates of VLDL secretion were defined by the slopes of the linear increases in plasma TG. (B) ELISA determination of the supernatant (left) and intracellular (right) VLDL levels in free fatty acids (FFA)-treated hepatocytes. $^{*}p<0.05$, $^{**}p<0.01$, $^{***}p<0.001$.

TET1 and MTTP were attenuated after triciribine treatment (Fig. 8B, C).

## Discussion

RASAL2 is a newly discovered metabolic regulator involved in energy homeostasis and adipogenesis. In recent years, a significant relationship between SNP rs10913469 (*SEC16B/RASAL2*) and obesity was found in Chinese, European, and American populations, and a lack of RASAL2 protects against obesity and metabolic disorders, including hepatic steatosis, in HFD-fed mice.[12–15] However, the specific role of RASAL2 in hepatic lipid metabolism remains undetermined. Here, we demonstrated that RASAL2 expression was up-regulated in both cellular and murine models of NAFLD and the livers of NAFLD patients. Further *in vivo* and *in vitro* experiments confirmed that RASAL2 directly and positively regulates hepatocellular lipid accumulation and that deficiency of RASAL2 ameliorates the hepatic steatosis induced by HFD feeding.

Increased hepatic TG accumulation is a result of increased uptake and *de novo* synthesis of FFA or decreased FFA oxidation and TG output, which involves a set of genes maintaining lipid homeostasis, including lipid absorption, biosynthesis, oxidation, and transport.[24] To elucidate the underlying mechanisms, we analyzed the expression levels of key genes regulating hepatic lipid metabolism in HFD-fed mice and found that the gene and protein expression levels of MTTP were significantly increased in RASAL2-deficient mice. *In vitro* experiments conducted in L02 and HepG2 cells further confirmed the results. As an endoplasmic reticulum-resident chaperone protein, MTTP is involved in the entire process and acts as the rate-limiting step in the assembly and secretion of hepatic VLDL.[25,26] MTTP ablation facilitates lipid accumulation in hepatocytes and aggravates hepatic steatosis in *ob/ob* mice.[27] As expected, the production and secretion rate of hepatic VLDL were markedly increased in RASAL2-deficient mice and hepatocytes with RASAL2 knockdown. Interestingly, the fasting plasma TG levels were lower in RASAL2-deficient mice than in WT littermates under HFD feeding conditions, which might be related to the lower body fat content and enhanced insulin sensitivity of RASAL2-deficient mice.

A key question that remains to be answered is how RASAL2 regulates the expression of MTTP. DNA methylation is well known to be involved in gene regulation and it is usually affected by host genetics and environmental factors.[28] DNA methylation disturbances have been implicated in hepatic steatosis, and altered DNA methylation was found to be associated with different stages of NAFLD.[29] Methylation at CpG site cg16213375 in the *FADS1* gene was strongly related to steatosis grade and fibrosis stage in the liver of obese patients.[29] The *MTTP* gene promoter

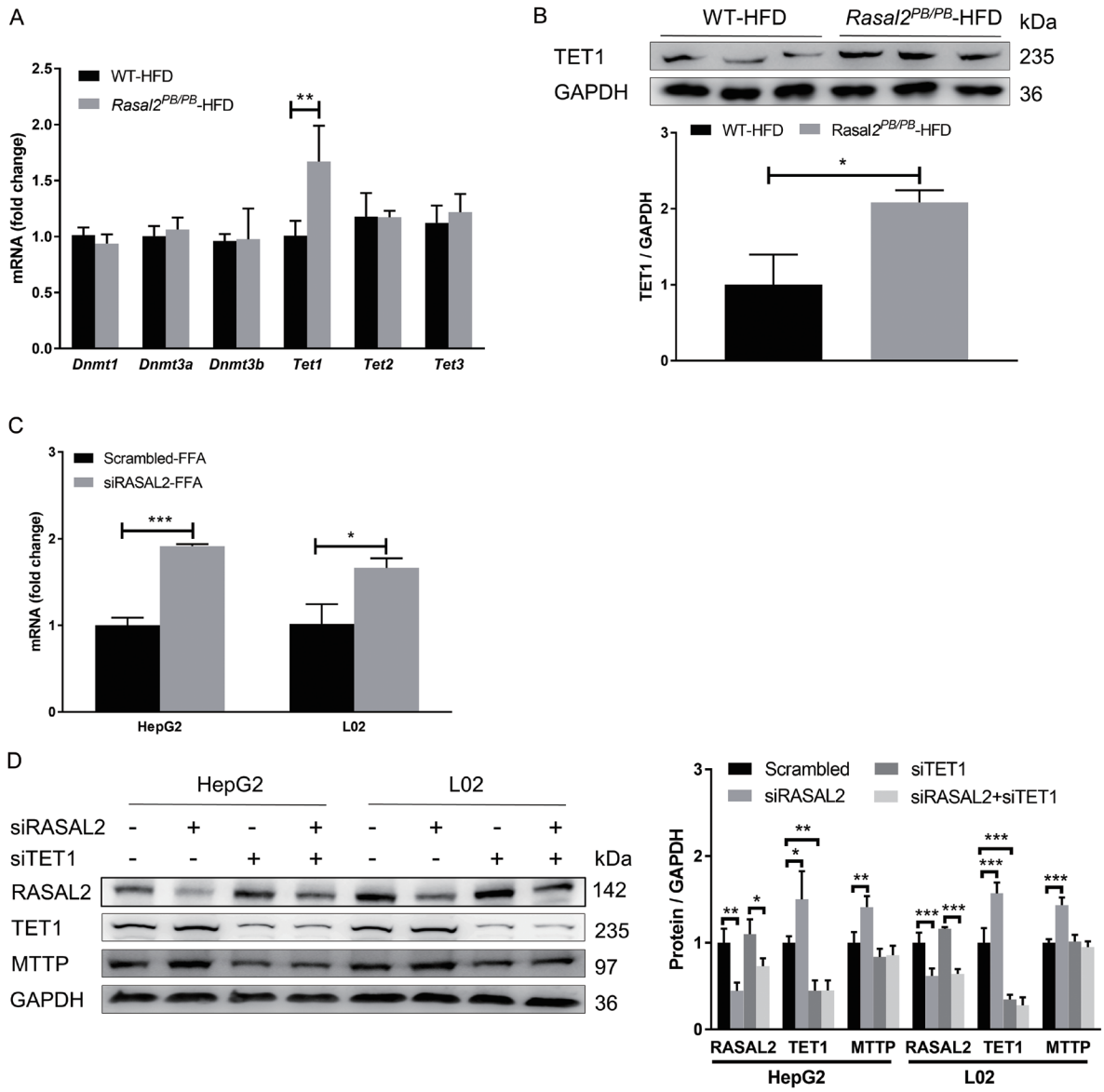


**Fig. 6. Increased expression of MTTP by RAS protein activator like 2 (RASAL2) deficiency is dependent on TET1.** (A) The mRNA expression of DNA methyltransferases and Tet family DNA demethylases in the livers of high-fat diet (HFD)-fed mice. (B) Protein expression of TET1 in the livers of RASAL2-deficient mice. (C) The mRNA expression of TET1 in RASAL2 knockdown hepatocytes. (D) Knocking down TET1 abolished the increased expression of MTTP in RASAL2 knockdown hepatocytes. $^{*}p<0.05$, $^{**}p<0.01$, $^{***}p<0.001$.

is rich in CpG sites, as revealed by the CpG island UCSC annotation database. We therefore speculated that RASAL2 regulated MTTP expression by DNA methylation in the HFD-induced mouse model of NAFLD. Indeed, it was found that the global 5-mC levels were reduced and the global 5-hmC levels were elevated in RASAL2 knockdown hepatocytes, and the expression level of TET1, a DNA demethylase enzyme, was significantly elevated in the livers of RASAL2 deficient mice and RASAL2 knockdown hepatocytes. Furthermore, TET1 directly bound to the *MTTP* gene promoter, and 5-hmC levels in the *MTTP* promoter region were significantly increased with the knockdown of RASAL2 in FFA-treated hepatocytes. Taken together, the results suggested that RASAL2 deficiency led to increased expression of TET1 and thus upregulated MTTP expression via TET1-mediated DNA hydroxymethylation.

The PI3K/AKT pathway is a major signaling effector downstream of activated Ras.[30] Once PI3K is activated, it is translocated from the cytoplasm to the plasma membrane where it phosphorylates PIP2 to PIP3, which then activates the downstream target AKT.[31–33] PI3K/AKT mediates numerous cellular functions, including energy metabolism, growth, motility, proliferation, and survival.[34] Previous studies have demonstrated that inhibition of AKT-dependent phosphorylation of FoxO1 results in reduced production of MTTP and hepatic VLDL, and PI3K/AKT/mTOR activity regulates the expression of TET family proteins and TET-mediated DNA hydroxymethylation during valproic acid-induced neural stem cell differentiation.[35,36] In the present study, higher levels of phosphorylated AKT were observed, and inhibition of the AKT pathway by triciribine obviously attenuated the upregulation of TET1 and MTTP in RASAL2

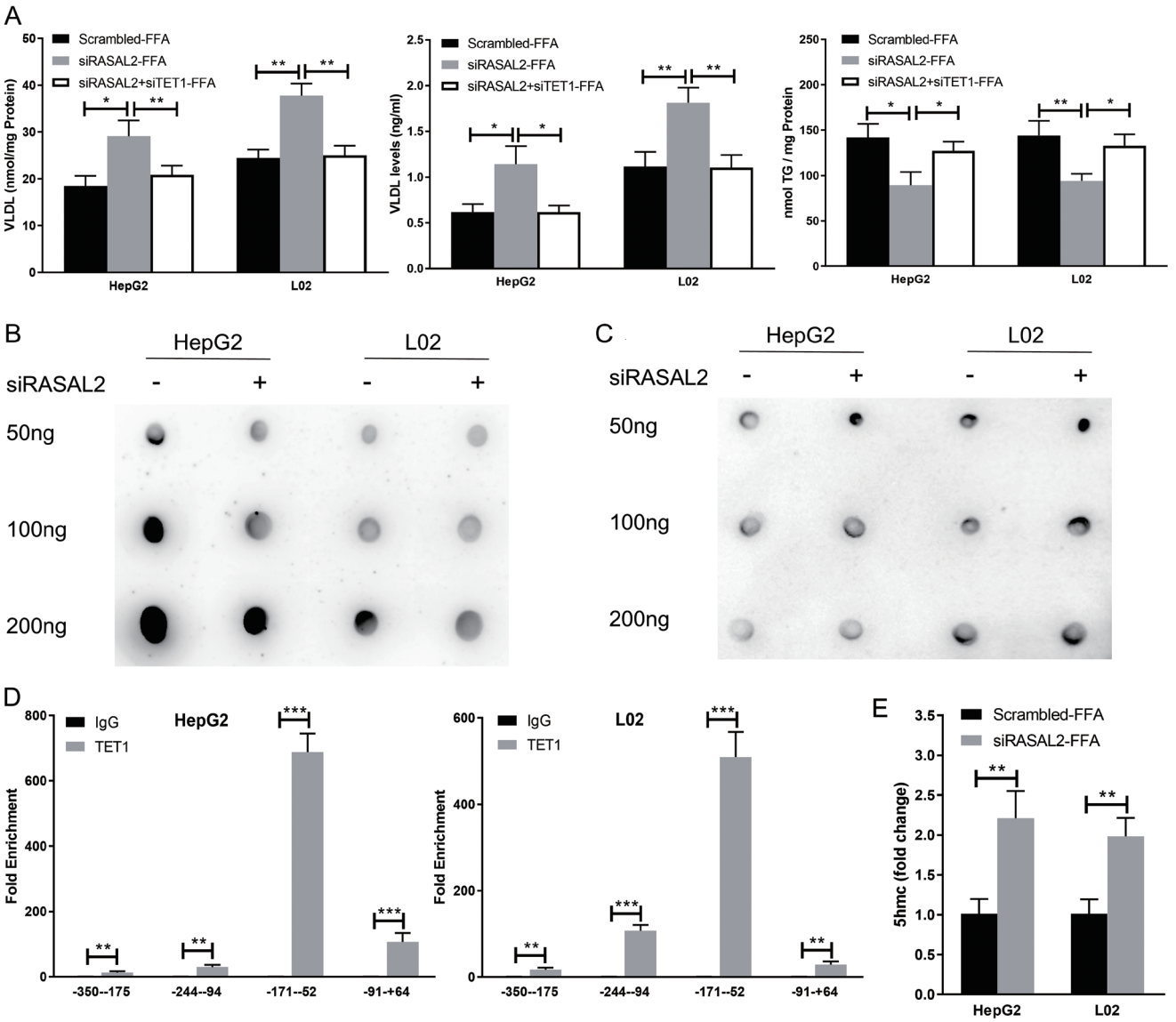


**Fig. 7. TET1 mediates MTTP upregulation by DNA hydroxymethylation in RAS protein activator like 2 (RASAL2) knockdown hepatocytes.** (A) Knocking down TET1 abolished the increased production and secretion of very low-density lipoprotein (VLDL) and restored free fatty acids (FFA)-induced lipid accumulation in RASAL2 knockdown hepatocytes. (B) Decreased global 5-methylcytosine (5-mC) levels in RASAL2 knockdown hepatocytes. (C) Increased global 5-hydroxymethylcytosine (5-hmC) levels in RASAL2 knockdown hepatocytes. (D) Chromatin immunoprecipitation (ChIP) experiment confirming the direct binding of TET1 to the *MTTP* promoter region. (E) Knockdown of RASAL2 increased DNA hydroxymethylation of the *MTTP* gene promoter in FFA-treated hepatocytes. $^{*}p<0.05$, $^{**}p<0.01$, $^{***}p<0.001$.

knockdown hepatocytes, indicating that the regulatory role of RASAL2 on TET1 and MTTP was mediated by the AKT signaling pathway.

In summary, this study demonstrated that RASAL2 deficiency increases hepatic production and secretion of VLDL and thus ameliorates hepatic steatosis through the AKT/TET1/MTTP axis (Fig. 8D). Several limitations need to be considered, including the use of whole-body knockout mice and the exclusion of female mice. It is difficult to determine whether RASAL2 deficiency in liver, adipose, or other tissues is the main cause of the phenotypes observed in global RASAL2 knockout mice. However, the results of this study highlight the importance of RASAL2 in hepatic lipid metabolism. These results provide novel insights and help better understand the pathogenesis of NAFLD. Targeting RASAL2 is a promising strategy for the treatment of NAFLD and its associated metabolic disorders.

## Funding

This work was supported by National Natural Science Foundation of China (grant number 82070591), Local Innovative and Research Teams Project of Guangdong Pearl River Talents Program (grant number 2017BT01S131), and Postdoctoral Science Foundation of China (grant number 2018M641919).

## Conflict of interest

The authors have no conflict of interests related to this pub-

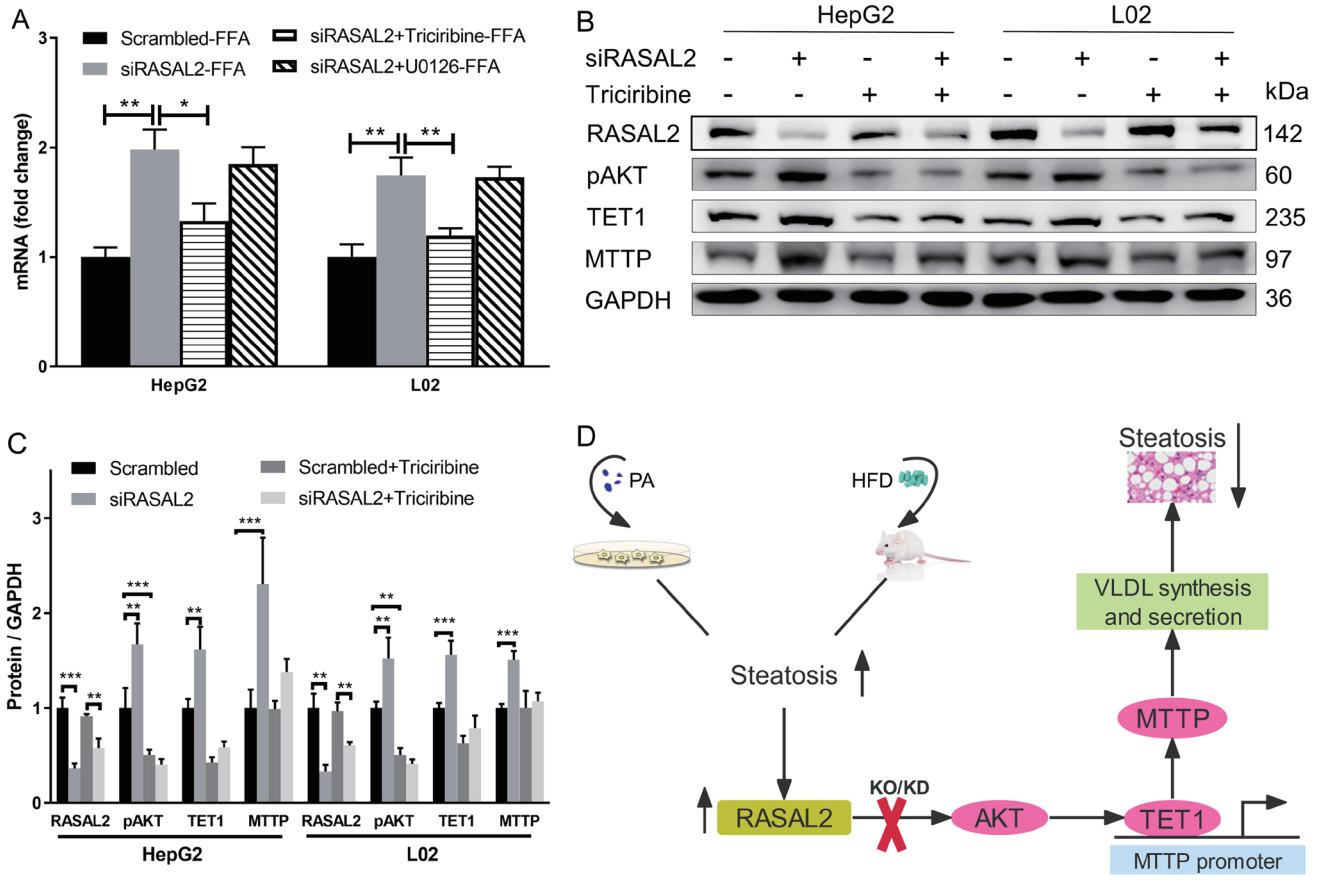


**Fig. 8. RAS protein activator like 2 (RASAL2) regulates TET1 expression through the AKT signaling pathway.** (A) Triciribine, an AKT inhibitor, abolished the increased gene expression of TET1 in RASAL2 knockdown hepatocytes. (B) Western blot analyses of the effects of triciribine on TET1 and MTTP expression in RASAL2 knockdown hepatocytes. (C) Densitometric quantification of the western blot results. (D) Schematic model depicting the mechanisms underlying the protective effect of RASAL2 deficiency on hepatic steatosis. $^{*}p<0.05$, $^{**}p<0.01$, $^{***}p<0.001$.

lication.

## Author contributions

Study concept and design (JL, JZ), acquisition of data (HD, JHY, GG), analysis and interpretation of data (HD, JHY, GG, YYM, JCW), drafting of the manuscript (HD), critical revision of the manuscript for important intellectual content (HD, JZ, JCW), and administrative, technical, or material support, study supervision (JL, JZ, JCW).

## Ethical statement

All animal study protocols were approved by the Committee on the Ethics of Animal Experiments of Fudan University and implemented according to the National Institutes of Health Guide for the Care and Use of Laboratory Animals. All tissue samples were obtained with informed consent following Institutional Review Board approval and following the ethical guidelines of the Declaration of Helsinki.

## Data sharing statement

No additional data are available.

## References

[1] Sun X, Seidman JS, Zhao P, Troutman TD, Spann NJ, Que X, *et al*. Neutralization of Oxidized Phospholipids Ameliorates Non-alcoholic Steatohepatitis. Cell Metab 2020;31(1):189–206.e8. doi:10.1016/j.cmet.2019.10.014, PMID:31761566.
[2] Younossi ZM, Koenig AB, Abdelatif D, Fazel Y, Henry L, Wymer M. Global epidemiology of nonalcoholic fatty liver disease-Meta-analytic assessment of prevalence, incidence, and outcomes. Hepatology 2016;64(1):73–84. doi:10.1002/hep.28431, PMID:26707365.
[3] Estes C, Anstee QM, Arias-Loste MT, Bantel H, Bellentani S, Caballeria J, *et al*. Modeling NAFLD disease burden in China, France, Germany, Italy, Japan, Spain, United Kingdom, and United States for the period 2016-2030. J Hepatol 2018;69(4):896–904. doi:10.1016/j.jhep.2018.05.036, PMID:29886156.
[4] Setiawan VW, Stram DO, Porcel J, Lu SC, Le Marchand L, Noureddin M. Prevalence of chronic liver disease and cirrhosis by underlying cause in understudied ethnic groups: The multiethnic cohort. Hepatology 2016;64:1969–1977. doi:10.1002/hep.28677, PMID:27301913.
[5] Kolachala VL, Palle S, Shen M, Feng A, Shayakhmetov D, Gupta NA. Loss of L-selectin-guided CD8+, but not CD4+, cells protects against ischemia reperfusion injury in a steatotic liver. Hepatology 2017;66(4):1258–1274. doi:10.1002/hep.29276, PMID:28543181.
[6] King PD, Lubeck BA, Lapinski PE. Nonredundant functions for Ras GTPase-activating proteins in tissue homeostasis. Sci Signal 2013;6(264):re1. doi:10.1126/scisignal.2003669, PMID:23443682.
[7] Huang Y, Zhao M, Xu H, Wang K, Fu Z, Jiang Y, *et al*. RASAL2 down-regulation in ovarian cancer promotes epithelial-mesenchymal transition and metastasis. Oncotarget 2014;5(16):6734–6745. doi:10.18632/oncotarget.2244, PMID:25216515.
[8] Hui K, Gao Y, Huang J, Xu S, Wang B, Zeng J, *et al*. RASAL2, a RAS GTPase-activating protein, inhibits stemness and epithelial-mesenchymal transition via MAPK/SOX2 pathway in bladder cancer. Cell Death Dis 2017;8(2):e2600. doi:10.1038/cddis.2017.9, PMID:28182001.
[9] Hui K, Yue Y, Wu S, Gu Y, Guan B, Wang X, *et al*. The expression and

function of RASAL2 in renal cell carcinoma angiogenesis. Cell Death Dis 2018;9(9):881. doi:10.1038/s41419-018-0898-x, PMID:30158581.
[10] Feng M, Bao Y, Li Z, Li J, Gong M, Lam S, *et al*. RASAL2 activates RAC1 to promote triple-negative breast cancer progression. J Clin Invest 2014; 124(12):5291–5304. doi:10.1172/JCI76711, PMID:25384218.
[11] Pan Y, Tong JHM, Lung RWM, Kang W, Kwan JSH, Chak WP, *et al*. RASAL2 promotes tumor progression through LATS2/YAP1 axis of hippo signaling pathway in colorectal cancer. Mol Cancer 2018;17(1):102. doi:10.1186/s12943-018-0853-6, PMID:30037330.
[12] Thorleifsson G, Walters GB, Gudbjartsson DF, Steinthorsdottir V, Sulem P, Helgadottir A, *et al*. Genome-wide association yields new sequence variants at seven loci that associate with measures of obesity. Nat Genet 2009;41(1):18–24. doi:10.1038/ng.274, PMID:19079260.
[13] Cheung CY, Tso AW, Cheung BM, Xu A, Ong KL, Fong CH, *et al*. Obesity susceptibility genetic variants identified from recent genome-wide association studies: implications in a chinese population. J Clin Endocrinol Meta 2010;95(3):1395–1403. doi:10.1210/jc.2009-1465, PMID:20061430.
[14] León-Mimila P, Villamil-Ramírez H, Villalobos-Comparán M, Villarreal-Molina T, Romero-Hidalgo S, López-Contreras B, *et al*. Contribution of common genetic variants to obesity and obesity-related traits in mexican children and adults. PLoS One 2013;8(8):e70640. doi:10.1371/journal.pone.0070640, PMID:23950976.
[15] Zhu X, Xie S, Xu T, Wu X, Han M. Rasal2 deficiency reduces adipogenesis and occurrence of obesity-related disorders. Mol Metab 2017;6(6):494–502. doi:10.1016/j.molmet.2017.03.003, PMID:28580280.
[16] Gómez-Lechón MJ, Donato MT, Martínez-Romero A, Jiménez N, Castell JV, O'Connor JE. A human hepatocellular in vitro model to investigate steatosis. Chem Biol Interact 2007;165(2):106–116. doi:10.1016/j.cbi.2006.11.004, PMID:17188672.
[17] Ye J, Li JZ, Liu Y, Li X, Yang T, Ma X, *et al*. Cideb, an ER- and lipid droplet-associated protein, mediates VLDL lipidation and maturation by interacting with apolipoprotein B. Cell Metab 2009;9(2):177–190. doi:10.1016/j.cmet.2008.12.013, PMID:19187774.
[18] Cvitanović Tomaš T, Urlep Ž, Moškon M, Mraz M, Rozman D. LiverSex Computational Model: Sexual Aspects in Hepatic Metabolism and Abnormalities. Front Physiol 2018;9:360. doi:10.3389/fphys.2018.00360, PMID:29706895.
[19] Raabe M, Véniant MM, Sullivan MA, Zlot CH, Björkegren J, Nielsen LB, *et al*. Analysis of the role of microsomal triglyceride transfer protein in the liver of tissue-specific knockout mice. J Clin Invest 1999;103(9):1287–1298. doi:10.1172/JCI6576, PMID:10225972.
[20] Chang X, Yan H, Fei J, Jiang M, Zhu H, Lu D, *et al*. Berberine reduces methylation of the MTTP promoter and alleviates fatty liver induced by a high-fat diet in rats. J Lipid Res 2010;51(9):2504–2515. doi:10.1194/jlr.M001958, PMID:20567026.
[21] Ito S, D'Alessio AC, Taranova OV, Hong K, Sowers LC, Zhang Y. Role of Tet proteins in 5mC to 5hmC conversion, ES-cell self-renewal and inner cell mass specification. Nature 2010;466(7310):1129–1133. doi:10.1038/nature09303, PMID:20639862.
[22] McLaughlin SK, Olsen SN, Dake B, De Raedt T, Lim E, Bronson RT, *et al*. The RasGAP gene, RASAL2, is a tumor and metastasis suppressor. Cancer Cell 2013;24(3):365–378. doi:10.1016/j.ccr.2013.08.004, PMID:24029233.
[23] Jia Z, Liu W, Gong L, Xiao Z. Downregulation of RASAL2 promotes the proliferation, epithelial-mesenchymal transition and metastasis of colorectal cancer cells. Oncol Lett 2017;13(3):1379–1385. doi:10.3892/ol.2017.5581, PMID:28454265.
[24] Liu C, Yang Z, Wu J, Zhang L, Lee S, Shin DJ, *et al*. Long noncoding RNA H19 interacts with polypyrimidine tract-binding protein 1 to reprogram hepatic lipid homeostasis. Hepatology 2018;67(5):1768–1783. doi:10.1002/hep.29654, PMID:29140550.
[25] Wang S, Chen Z, Lam V, Han J, Hassler J, Finck BN, *et al*. IRE1α-XBP1s induces PDI expression to increase MTP activity for hepatic VLDL assembly and lipid homeostasis. Cell Metab 2012;16(4):473–486. doi:10.1016/j.cmet.2012.09.003, PMID:23040069.
[26] Gong Z, Su K, Cui L, Tas E, Zhang T, Dong HH, *et al*. Central effects of humanin on hepatic triglyceride secretion. Am J Physiol Endocrinol Metab 2015;309(3):E283–292. doi:10.1152/ajpendo.00043.2015, PMID:26058861.
[27] Stefano JT, de Oliveira CP, Corrêa-Giannella ML, de Lima VM, de Sá SV, de Oliveira EP, *et al*. Nonalcoholic steatohepatitis (NASH) in ob/ob mice treated with yo jyo hen shi ko (YHK): effects on peroxisome proliferator-activated receptors (PPARs) and microsomal triglyceride transfer protein (MTP). Dig Dis Sci 2007;52(12):3448–3454. doi:10.1007/s10620-007-9810-8, PMID:17394061.
[28] Yang Y, Wu L, Shu X, Lu Y, Shu XO, Cai Q, *et al*. Genetic Data from Nearly 63,000 Women of European Descent Predicts DNA Methylation Biomarkers and Epithelial Ovarian Cancer Risk. Cancer Res 2019;79(3):505–517. doi:10.1158/0008-5472.CAN-18-2726, PMID:30559148.
[29] Walle P, Männistö V, de Mello VD, Vaittinen M, Perfilyev A, Hanhineva K, *et al*. Liver DNA methylation of FADS2 associates with FADS2 genotype. Clin Epigenetics 2019;11(1):10. doi:10.1186/s13148-019-0609-1, PMID:30654845.
[30] Zhang X, Qi Z, Yin H, Yang G. Interaction between p53 and Ras signaling controls cisplatin resistance via HDAC4- and HIF-1α-mediated regulation of apoptosis and autophagy. Theranostics 2019;9(4):1096–1114. doi:10.7150/thno.29673, PMID:30867818.
[31] Nussinov R, Jang H, Tsai CJ, Cheng F. Review: Precision medicine and driver mutations: Computational methods, functional assays and conformational principles for interpreting cancer drivers. PLoS Comput Biol 2019;15(3):e1006658. doi:10.1371/journal.pcbi.1006658, PMID:30921324.
[32] Pearson JRD, Regad T. Targeting cellular pathways in glioblastoma multiforme. Signal Transduct Target Ther 2017;2:17040. doi:10.1038/sigtrans.2017.40, PMID:29263927.
[33] Kim SB, Dent R, Im SA, Espié M, Blau S, Tan AR, *et al*. Ipatasertib plus paclitaxel versus placebo plus paclitaxel as first-line therapy for metastatic triple-negative breast cancer (LOTUS): a multicentre, randomised, double-blind, placebo-controlled, phase 2 trial. Lancet Oncol 2017;18(10):1360–1372. doi:10.1016/S1470-2045(17)30450-3, PMID:28800861.
[34] Soler A, Figueiredo AM, Castel P, Martin L, Monelli E, Angulo-Urarte A, *et al*. Therapeutic Benefit of Selective Inhibition of p110α PI3-Kinase in Pancreatic Neuroendocrine Tumors. Clin Cancer Res 2016;22(23):5805–5817. doi:10.1158/1078-0432.CCR-15-3051, PMID:27225693.
[35] Kamagate A, Qu S, Perdomo G, Su D, Kim DH, Slusher S, *et al*. FoxO1 mediates insulin-dependent regulation of hepatic VLDL production in mice. J Clin Invest 2008;118(6):2347–2364. doi:10.1172/JCI32914, PMID:18497885.
[36] Zhang X, He X, Li Q, Kong X, Ou Z, Zhang L, *et al*. PI3K/AKT/mTOR Signaling Mediates Valproic Acid-Induced Neuronal Differentiation of Neural Stem Cells through Epigenetic Modifications. Stem Cell Reports 2017;8(5):1256–1269. doi:10.1016/j.stemcr.2017.04.006, PMID:28494938.